Functional and Morphological Correlates of Connexin50 Expressed in *Xenopus laevis* Oocytes

Guido A. Zampighi,*‡ Donald D.F. Loo,‡ Michael Kreman,* Sepehr Eskandari,‡ and Ernest M. Wright‡

From the *Department of Neurobiology and ‡Department of Physiology, University of California, Los Angeles, School of Medicine, Los Angeles, California 90095

ABSTRACT Electrophysiological and morphological methods were used to study connexin50 (Cx50) expressed in *Xenopus laevis* oocytes. Oocytes expressing Cx50 exhibited a new population of intramembrane particles (9.0 nm in diameter) in the plasma membrane. The particles represented hemichannels (connexin hexamers) because (a) their cross-sectional area could accommodate 24 ± 3 helices, (b) when their density reached 300–400/μm^2, they formed complete channels (dodecamers) in single oocytes, and assembled into plaques, and (c) their appearance in the plasma membrane was associated with a whole-cell current, which was activated at low external Ca^{2+} concentration ($[Ca^{2+}]_o$), and was blocked by octanol and by intracellular acidification. The Cx50 hemichannel density was directly proportional to the magnitude of the Cx50 Ca^{2+}-sensitive current. Measurements of hemichannel density and the Ca^{2+}-sensitive current in the same oocytes suggested that at physiological $[Ca^{2+}]_o$ (1–2 mM), hemichannels rarely open. In the cytoplasm, hemichannels were present in ~0.1-μm diameter "coated" and in larger 0.2–0.5-μm diameter vesicles. The smaller coated vesicles contained endogenous plasma membrane proteins of the oocyte intermingled with 5–40 Cx50 hemichannels, and were observed to fuse with the plasma membrane. The larger vesicles, which contained Cx50 hemichannels, gap junction channels, and endogenous membrane proteins, originated from invaginations of the plasma membrane, as their lumen was labeled with the extracellular marker peroxidase. The insertion rate of hemichannels into the plasma membrane (80,000/s), suggested that an average of 4,000 small coated vesicles were inserted every second. However, insertion of hemichannels occurred at a constant plasma membrane area, indicating that insertion by vesicle exocytosis (60–500 μm^2 membranes/s) was balanced by plasma membrane endocytosis. These exocytotic and endocytotic rates suggest that the entire plasma membrane of the oocyte is replaced in ~24 h.

KEY WORDS: connexins • hemichannels • gap junctions • exocytosis • endocytosis

introduction

A family of integral membrane proteins, called connexins, forms specialized cell–cell channels that serve as intercellular pathways of chemical and electrical information transmission. The cell–cell channel is assembled from the docking of two hemichannels (i.e., connexin hexamers) located in the plasma membrane of adjacent cells. This mechanism of cell–cell channel assembly suggests that there may be pools of hemichannels in the plasma membrane of participating cells. Although the physiological significance of undocked hemichannels in cell permeability and homeostasis is unclear, evidence has accumulated that hemichannels can function independently as non- or cation-selective, large conductance ion channels whose activity is dependent on the extracellular calcium concentration and intracellular pH (DeVries and Schwartz, 1992; Ebihara, 1996). Cloning of the connexins, together with the introduction of efficient expression systems such as *Xenopus laevis* oocytes, opened new experimental avenues to study connexin hemichannels. While the expression of all connexins in oocytes leads to the formation of functional cell–cell channels by paired oocytes (e.g., Werner et al., 1985; Dahl et al., 1987; Steiner and Ebihara, 1996; Wang and Peracchia, 1998), only a few connexins form functional hemichannels in the plasma membrane (Paul et al., 1991; Ebihara and Steiner, 1993; Gupta et al., 1994; Ebihara et al., 1995; Ebihara, 1996; Trexler et al., 1996).

Here, we have combined electron microscopic and electrophysiological methods (Zampighi et al., 1995) to study mouse connexin50 (Cx50)[1] expressed in *Xenopus* oocytes. Our approach combines hemichannel functional assays and the determination of the number of hemichannels in the plasma membrane of the same cell to assess the contribution of these channels to cell conductance. We show that expression of Cx50 in oocytes led to the insertion of functional hemichannels into the plasma membrane. Measurements of the total

Address correspondence to Guido A. Zampighi, Department of Neurobiology, UCLA School of Medicine, 10833 Le Conte Avenue, CHS, Box 951763, Los Angeles, CA 90095-1763. Fax: 310-825-2224; E-mail: gzampighi@mednet.ucla.edu

[1]*Abbreviations used in this paper:* Cx50, connexin50; I–V, current–voltage.

number of hemichannels in the plasma membrane and the Cx50 current in the same oocytes suggested that hemichannels rarely open at physiological calcium concentrations. When the density of hemichannels in the plasma membrane reached 300–400/μm^2, they formed complete channels (dodecamers) and assembled into gap junctional plaques. The morphological studies further allowed the identification of hemichannels in vesicles shuttled to and from the plasma membrane. In the cytoplasm, hemichannels were present in small ($\sim$0.1-μm diameter) "coated" and in larger (0.2–0.5-μm diameter) vesicles. The coated vesicles fused with the plasma membrane, whereas the larger vesicles originated from endocytosis of the plasma membrane. Trafficking of Cx50 hemichannels took place without changing the area of the plasma membrane, indicating that the rate of vesicles insertion into the plasma membrane was balanced by the rate of vesicle retrieval.

materials and methods

Oocytes

Mature *Xenopus laevis* oocytes were injected with 50 nl distilled water or 50 nl 1 μg/μl mouse Cx50 cRNA (White et al., 1992), and incubated at 18°C in Barth's medium (mM: 88 NaCl, 1 KCl, 0.33 $Ca(NO_3)_2$, 0.41 $CaCl_2$, 0.82 $MgSO_4$, 2 $NaHCO_3$, and 10 HEPES/Tris, pH 7.4) containing 0.1 mg/ml gentamicin (Parent et al., 1992; Zampighi et al., 1995).

Electrophysiology

Electrophysiological experiments were performed with a two-electrode voltage-clamp technique (Loo et al., 1993). Oocytes were placed in a NaCl buffer (mM: 100 NaCl, 2 KCl, 1 $CaCl_2$, 1 $MgCl_2$, and 10 HEPES/Tris, pH 7.5) and the membrane potential was held at −50 mV. The whole-cell Cx50 currents were induced by varying the concentration of external calcium ($[Ca^{2+}]_o$). The Ca^{2+} concentration was adjusted as desired by adding appropriate amounts of Ca^{2+} and EGTA (Findlay et al., 1985). To obtain current–voltage (I–V) relations, the pulse protocol consisted of 1,000-ms voltage steps from a holding potential (V_h) of −50 mV to a series of test voltages from +50 to −150 mV in 20-mV decrements (pCLAMP; Axon Instruments). The voltage clamp had a settling time of 0.2–0.8 ms. Currents were low-pass filtered at 500 Hz, and sampled at 1 ms per point. Membrane capacitance measurements were used to estimate the total surface area of the plasma membrane (using 1 $\mu F/cm^2$; see Loo et al., 1993; Zampighi et al., 1995). The capacitance was determined by applying 10–20-mV test pulses (V_t) of 30–100-ms duration from the holding potential (−50 mV). At each test voltage, the charge (Q) was obtained by integration of the capacitive transient. In both control and Cx50-expressing oocytes, capacitive transients showed a single time constant ($\sim$1 ms), and Q was a linear function of the voltage step ($V_t - V_h$). The slope of the Q versus ($V_t - V_h$) relation was the membrane capacitance C_m. In oocytes expressing Cx50, capacitance measurements were made at 5 mM $[Ca^{2+}]_o$ to avoid hemichannel activation. Membrane conductance was obtained as either the slope of the steady state I–V relationship or, where indicated, as a chord conductance (e.g., see Fig. 9). The reversal potential (V_{rev}) was determined by subtracting the endogenous currents at 5 mM $[Ca^{2+}]_o$. All experiments were performed at 21 ± 1°C.

Fixation

After functional measurements, oocytes were fixed at room temperature and prepared for morphological studies (Zampighi et al., 1995). The fixative solution contained 3–3.5% glutaraldehyde in 0.2 M Na-cacodylate (pH 7.35).

Thin Sectioning

Oocytes were postfixed in 1% OsO_4 in 0.2 M Na-cacodylate buffer for 90 min at room temperature. They were washed in 0.1 M Na-acetate buffer (pH 5.0) and block-stained in 0.5% uranyl acetate in 0.1 M Na-acetate buffer (pH 5.0) overnight at 4°C. They were dehydrated in ethanol, passed through propylene oxide, and embedded in Polybed 812. Sections were cut in a Sorval MT5000 ultramicrotome (Dupont), collected on single-hole formvar-coated grids, and stained with uranyl acetate and lead (Zampighi et al., 1988).

Peroxidase

Control oocytes and oocytes injected with cRNA were incubated for 1 h in Barth's solution containing 0.5–1.5 mg/ml of peroxidase (Sigma Chemical Co.), and were then fixed in 3–3.5% glutaraldehyde in 0.2 M Na-cacodylate (pH 7.35) for 2 h at room temperature. They were washed and incubated in 0.1 mg/ml diaminobenzidine in 0.1 M Tris/HCl (pH 7.5) and H_2O_2, and then prepared for thin sectioning.

Freeze Fracture

Fixed oocytes were infiltrated with 25% glycerol in 0.2 M Na-cacodylate (pH 7.35) for 1 h (21 ± 1°C). Each oocyte was cut into six to eight small pieces ($\sim$1 mm^3) to obtain replicas from different regions of the surface of the oocyte. The pieces were placed on Balzers specimen holders with the external surface (i.e., the vitelline membrane) facing upward. This orientation yielded extensive P face areas of the plasma membrane, which allowed us to determine the density and size of the newly inserted particles (Zampighi et al., 1995; Eskandari et al., 1998). The specimens were frozen by immersion in liquid propane maintained just above freezing in a liquid nitrogen bath. The frozen specimens were transferred to a Balzers 400 K freeze-fracture-etch apparatus, fractured at either −150° or −120°C at $\sim 10^{-7}$ mbar of partial pressure. The fractured surfaces were coated with platinum at 80°C and carbon at 90°C. Replication at 80°C decreased the length of the shadow of the particle, which greatly facilitated the density quantification and the measurement of the particle diameter. The specimens were coated with 0.5% collodion in amyl acetate to avoid fragmentation of the replica, and cleaned in a solution of bleach to dissolve the organic material. The replicas were washed in distilled water and deposited on formvar-coated, single-hole copper grids. The collodion was removed by immersion in amyl acetate (Zampighi et al., 1988).

Sampling

The large area of the oocyte plasma membrane ($\sim 3 \times 10^7$ μm^2) introduced sampling difficulties since only a small percentage of the area ($6–8 \times 10^2$ μm^2) was imaged and used for the determination of the particle density. To address this, P faces collected from three to four replicas from different regions of the plasma membrane of each oocyte were imaged at 25,000×. Approximately 100 negatives were collected from each replica. From this pool, $\sim$20 negatives per replica free of optical aberrations and containing an area of 1–2 μm^2 of uninterrupted P fracture face were printed and used for quantification (Table I). Altogether, the data were obtained by studying over 1,000 negatives from

table i

Sampling of Morphological Data

Oocyte*	Number of replicas	Area quantified	Number of particles counted
		$\mu m^{2‡}$	
Control	3	17.5 (8)	3369
6	3	19.8 (11)	4342
24	4	21.5 (15)	8926
48	4	28.0 (12)	16455
72	3	19.2 (11)	14829
96	3	9.3 (6)	6038

*The duration of incubation after cRNA injection is given in hours. ‡For each oocyte, the total area quantified was the sum of the P face areas imaged from three to five replicas from different regions of the plasma membrane. The number in parentheses corresponds to the number of P face areas used in the quantification.

replicas of the fracture faces of the plasma membrane of control oocytes and oocytes injected with Cx50 cRNA. In replicas obtained from different poles of Cx50-expressing oocytes (vegetal versus animal), no differences were observed in the Cx50 hemichannel density or the fractional area covered by gap junction plaques.

Quantification

The images were enlarged to 75,000×, digitized, and analyzed using IMAGE software (National Institutes of Health). In each image, we measured the area of the P face and the total number of particles contained in that area. The particle density in the microvilli plasma membrane was quantified independently to ensure that it was similar to that of other regions of the plasma membrane. The diameter of the intramembrane particles was measured perpendicular to the direction of the shadow directly from negatives using a Profile Projector (6C; Nikon Inc.) at a final magnification of 250,000× (Eskandari et al., 1998).

The number of hemichannels in gap junction plaques (n_{gj}) was estimated using $n_{gj} = K A_t 2d$, where K is the fractional area covered by plaques per 100 μm^2 of plasma membrane, A_t is the total area of the plasma membrane calculated from the capacitance, d is the mean density of particles in plaques (9,196 ± 694/μm^2), and 2 because each gap-junction particle is composed of two hemichannels.

Resolution of the Method Used to Determine Particle Density

The density of endogenous P face particles in the plasma membrane of control oocytes was 196 ± 9 particles/μm^2 (mean ± SEM, $n = 8$, n refers to the number of P face regions from which the particles were sampled). To detect the expression of Cx50, the particle density had to increase at least to 250/μm^2; i.e., 54 particles/μm^2 (two SDs) above the mean particle density of control oocytes, which represents a confidence level of ~98%. The highest density at which each particle could be resolved without interference from the shadows of neighboring particles was ~10,000 particles/μm^2 (approached in gap junctional plaques).

results

Electrophysiology

Steady state properties of Cx50 hemichannels. The electrophysiological properties of *Xenopus laevis* oocytes injected with Cx50 cRNA were dependent on $[Ca^{2+}]_o$. When measured 3 d after injection, in 1 mM external Ca^{2+}, the resting membrane potential of Cx50-expressing oocytes was significantly different from that of control oocytes. Control oocytes had a resting potential of –50 ± 5 mV (mean ± SEM, $n = 5$) and a membrane conductance of 1.7 ± 0.2 μS ($n = 5$), while the resting potential of oocytes injected with Cx50 cRNA was −33 ± 2 mV ($n = 7$), and the membrane conductance was 7.2 ± 0.8 μS ($n = 7$). When the $[Ca^{2+}]_o$ was elevated to 5 mM, the resting membrane potential and conductance of Cx50-expressing oocytes were restored to those of the controls (not shown).

The dependence of the membrane conductance of oocytes expressing Cx50 on $[Ca^{2+}]_o$ was studied under voltage-clamp conditions. Fig. 1 A (top) shows a continuous current record from an oocyte expressing Cx50 and maintained at a holding potential (V_h) of −50 mV. Reduction in $[Ca^{2+}]_o$ from 1 mM to 10 μM induced an inward current of ~1,450 nA. This inward current was reversibly blocked (~65%) by intracellular acidification by addition of acetate (50 mM equimolar Na-acetate replacement for NaCl, pH 7.5) to the bathing medium. The current returned to baseline after restoration of $[Ca^{2+}]_o$ to 1 mM.

The response of control oocytes to the same experimental protocol is illustrated in Fig. 1 A (bottom). Reduction of $[Ca^{2+}]_o$ from 1 mM to 10 μM induced a small outward current (9 ± 3 nA, $n = 27$), which was insensitive to intracellular acidification. This experiment was repeated in more than 70 control oocytes and in none was there a Ca^{2+}-sensitive current as that detected in the Cx50-expressing cells. This suggests the absence of endogenous connexin hemichannels in our control oocytes.[2]

A feature of gap junction channels is their inhibition by octanol, heptanol, and halothane (Johnston et al., 1980; for review, see Spray and Burt, 1990). We tested the effect of 1-octanol on the currents activated by low $[Ca^{2+}]_o$. Fig. 1 B shows a current trace from an oocyte

[2]Other studies have reported currents activated at low $[Ca^{2+}]_o$ in control oocytes. One group concluded that these are Cl^- currents (Weber et al., 1995; Reifarth et al., 1997), and two groups concluded that these are nonselective cation currents through hemi-gap-junction channels (Ebihara, 1996; Zhang et al., 1998). Over a 4-yr period, we have not observed such currents in control oocytes under our experimental protocols. Furthermore, extensive examination of freeze-fracture replicas of the plasma membrane of control oocytes have not revealed particles resembling connexin hemichannels (i.e., a particle with a symmetrical cross-sectional geometry and a diameter of 6.5 nm). However, we consistently see such particles in oocytes expressing connexin50 or connexin46. These two independent lines of evidence lead us to the conclusion that endogenous oocyte connexins (i.e., connexin38) are not expressed at any significant level in the oocytes used in our studies. The reason for differences in the expression of endogenous connexin hemichannels in our oocytes and those of others is not immediately obvious.

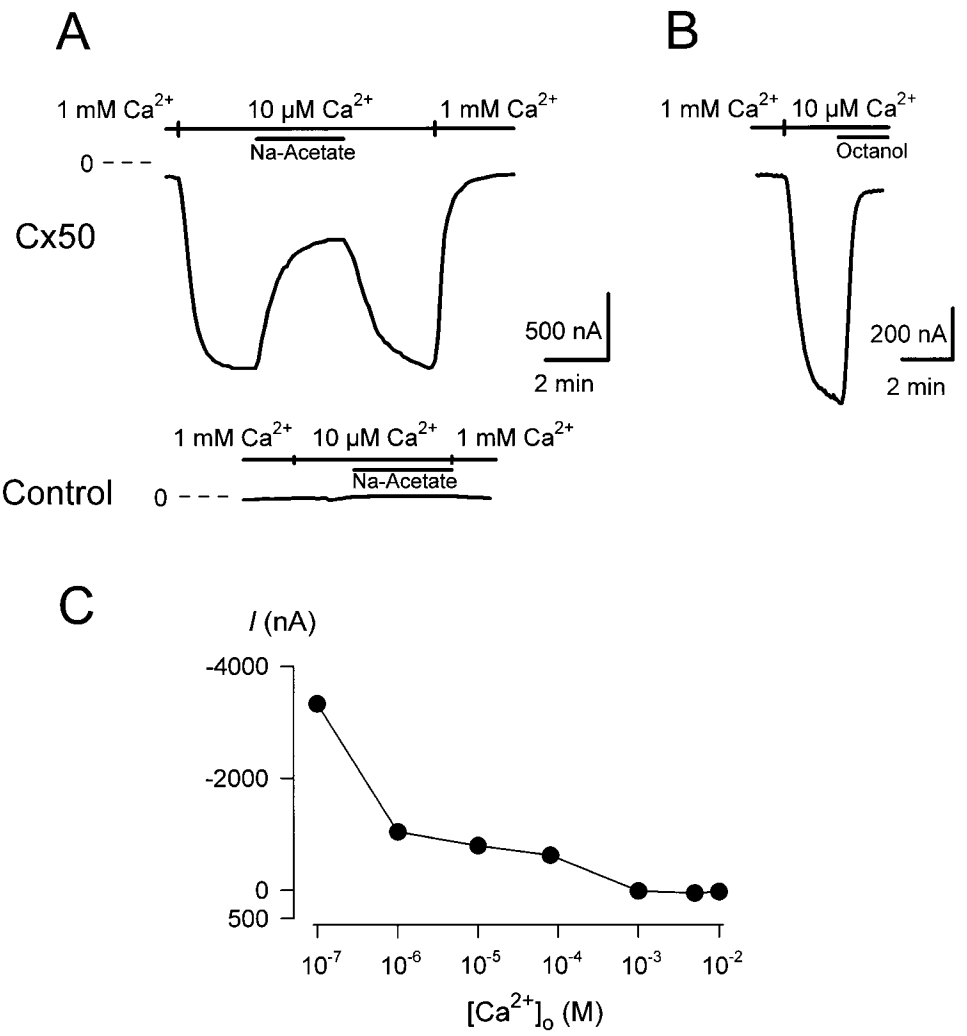

FIGURE 1. Cx50 hemichannels are sensitive to $[Ca^{2+}]_o$, intracellular pH, and octanol. (A) In a Cx50-expressing oocyte voltage-clamped at −50 mV (top), reduction of $[Ca^{2+}]_o$ from 1 mM to 10 μM induced a large inward current (I_{Cx50}). Intracellular acidification by the addition of 50 mM Na-acetate to the bathing medium resulted in an ~65% reversible inhibition of I_{Cx50}. In control oocytes (bottom), reduction of $[Ca^{2+}]_o$ or intracellular acidification had no appreciable effect on the current. (B) I_{Cx50} was inhibited by addition of 1 mM 1-octanol to the bathing medium. (C) The magnitude of I_{Cx50} depended on $[Ca^{2+}]_o$. Measurements were made 48 h after cRNA injection.

held at −50 mV. Reduction in $[Ca^{2+}]_o$ to 10 μM led to an inward current of ~900 nA that was reversibly inhibited by ~95% by addition of 1 mM octanol to the bathing medium. Octanol had no effect on the holding current of control oocytes (not shown).

We further studied the Ca^{2+} sensitivity of the inward current at −50 mV (Fig. 1 C). From 10^{-2} to 10^{-6} M $[Ca^{2+}]_o$, there were small incremental increases in the holding current; however, when $[Ca^{2+}]_o$ was lowered to 10^{-7} M, the current increased by ~3.3-fold (Fig. 1 C). In Ca^{2+}-free solutions (10 mM EGTA and 0 Ca^{2+}), the Cx50 currents were too large for reliable control of the membrane potential.

Voltage dependence of Cx50 hemichannels. In control oocytes, when the membrane potential was stepped from the holding (−50 mV) to test voltages, the capacitive transient decayed to a steady state with a time constant of ~1 ms (Fig. 2 A; Parent et al., 1992). This relaxation was independent of the $[Ca^{2+}]_o$ (data not shown). The steady state I–V relations in 5 mM or 10 μM external Ca^{2+} were similar (Fig. 2 A). Membrane conductances in 5 mM and 10 μM external Ca^{2+} in the oocyte in Fig. 2 A were 1.2 ± 0.1 and 1.3 ± 0.1 μS.

The current response of Cx50-expressing oocytes after step changes in membrane potential depended on $[Ca^{2+}]_o$ (Fig. 2 B). In 5 mM $[Ca^{2+}]_o$, the currents were not appreciably different from control oocytes, and the conductance was 2.4 ± 0.1 μS. In 10 μM $[Ca^{2+}]_o$, large Cx50 currents resulted that, after the initial capacitive transient, decayed slowly to a steady state (Fig. 2 B). At steady state, the inactivation was dependent on $[Ca^{2+}]_o$ (not shown) and the magnitude of the voltage step. It was most prominent at low $[Ca^{2+}]_o$ and at the largest voltage steps (Fig. 2 B). At the smallest voltage steps, there was no apparent inactivation as the relaxation of the current transient was not appreciably different from that of the capacitive transient, but at the largest voltage steps (±100 mV), the time constant of inactivation ranged from 220–300 ms.

The Cx50 I–V relationships were measured at 10 ($I_{initial}$) and 980 ($I_{steady\text{-}state}$) ms after the onset of the voltage pulse (Fig. 2 C). $I_{initial}$ was proportional to the size of

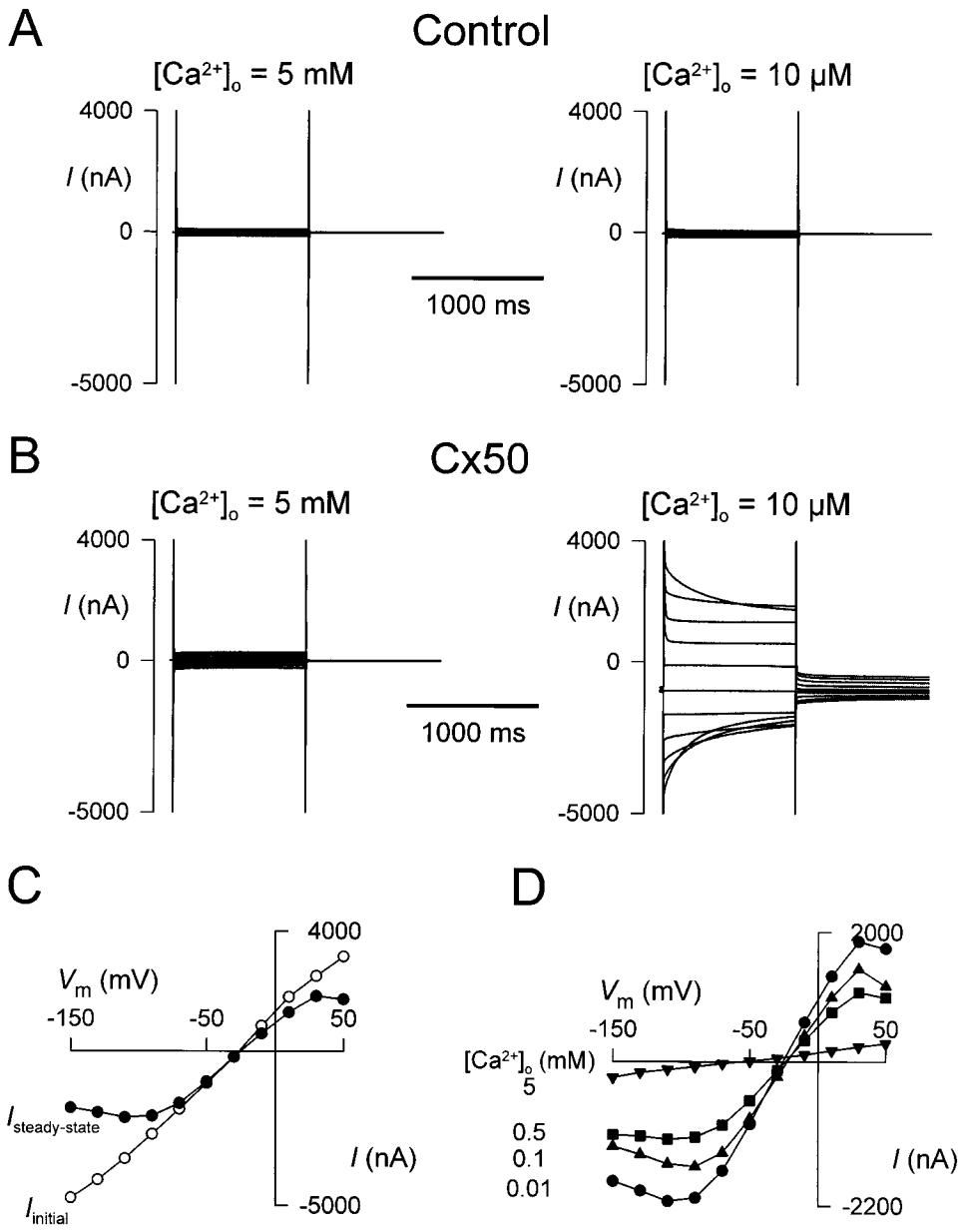

FIGURE 2. Voltage dependence of Cx50 Ca^{2+}-sensitive currents. (A) In control oocytes, no Ca^{2+}-sensitive currents were observed when $[Ca^{2+}]_o$ was lowered (see also Fig. 1 A). The capacitive transient had a single time constant of ~1 ms. (B) Oocytes expressing Cx50 exhibited large Ca^{2+}-sensitive currents (I_{Cx50}) at 10 μM $[Ca^{2+}]_o$. (C) I_{Cx50} at 10 ms ($I_{initial}$) (○) and 980 ms ($I_{steady\text{-}state}$) (●) after the onset of the voltage pulse. V_{rev} was the same for both currents (−25 mV). (D) $I_{steady\text{-}state}$–V at various $[Ca^{2+}]_o$. The data in B–D were obtained from the same oocyte, and those in A and B were obtained from an oocyte from the same batch. Data obtained from over several hundred control and Cx50-expressing oocytes were similar to those reported here.

the voltage step, resulting in a near linear I–V relationship. $I_{steady\text{-}state}$ deviated from linearity and at the extreme voltage steps (−150 to −90 mV and +30 to +50 mV), the conductance was negative. Membrane conductance was 41 ± 1 μS for $I_{initial}$ (−150 to +50 mV) and 35 ± 1 μS for $I_{steady\text{-}state}$ (−70 to +30 mV). Both $I_{initial}$ and $I_{steady\text{-}state}$ reversed at the same membrane potential (−25 mV), indicating that they were carried by the same ionic species. Equimolar (100 mM) replacement of external Na^+ with choline shifted V_{rev} for both currents to more negative values (approximately −35 mV). V_{rev} was not significantly affected by replacement of external Cl^- with gluconate or Mes (not shown) or by variations in $[Ca^{2+}]_o$ (Fig. 2 D).

Therefore, in oocytes expressing Cx50, the functional and pharmacological properties of the current induced at low $[Ca^{2+}]_o$ were consistent with the expression of a functional connexin hemichannel and, henceforth, this current will be referred to as I_{Cx50}.

Time course of Cx50 expression and membrane capacitance. I_{Cx50} was used as a functional assay of the presence of Cx50 in the plasma membrane. The magnitude of I_{Cx50} was dependent on the length of time after cRNA injection (Fig. 3 A). I_{Cx50} appeared as early as ~3 h after injection (data not shown), increased steadily up to the third day and, thereafter, decreased (Fig. 3 A, ●). Although this time course was very reproducible, the magnitude of I_{Cx50} was dependent on the amount of cRNA injected and the frog from which the oocytes were harvested. Control oocytes (V_h = −50 mV) did not exhibit a Ca^{2+}-sensitive current over this time course (Fig. 3 A, ○).

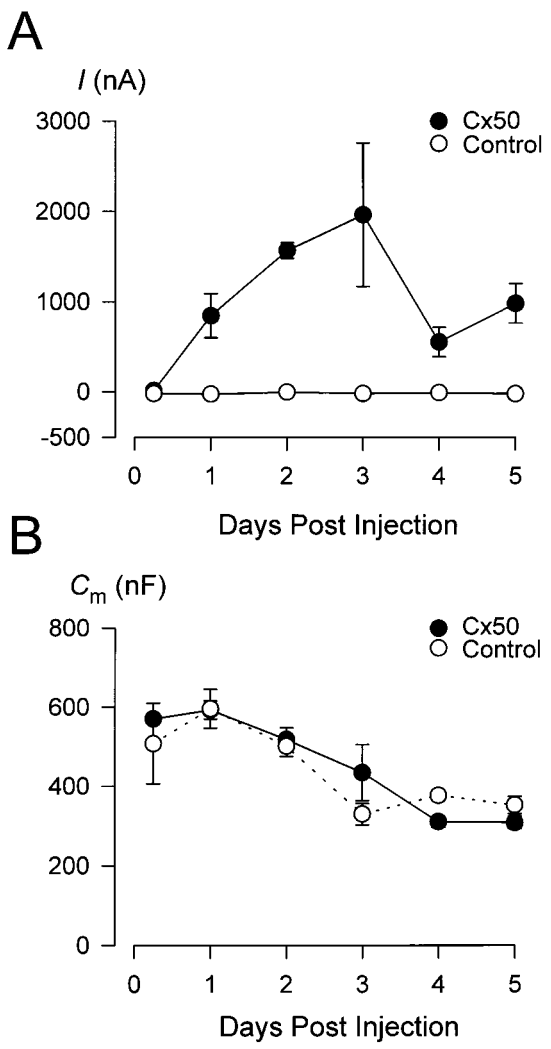

FIGURE 3. Time course of I_{Cx50} and membrane capacitance (C_m) as a function of Cx50 expression. (A) The magnitude of Ca^{2+}-sensitive currents of control oocytes (○) and I_{Cx50} in oocytes expressing Cx50 (●) 6 h to 5 d after cRNA injection. V_h was −50 mV and the Ca^{2+}-sensitive current was assessed as the difference in the holding current when the $[Ca^{2+}]_o$ was changed from 5 mM to 10 μM. (B) C_m of control oocytes (○, dotted line) and oocytes expressing Cx50 (●, solid line) is shown as a function of the time after water or cRNA injection. In both A and B, each data point represents the mean of measurements obtained from three to five different oocytes from the same batch, and the entire protocol was repeated with three different batches of oocytes.

The membrane capacitance (C_m) of oocytes injected with Cx50 cRNA was not different from that of control oocytes up to 5 d (300–600 nF). In both groups of oocytes, C_m remained unchanged up to the third day and decreased thereafter (Fig. 3 B). Thus, Cx50 expression occurred without altering the plasma membrane area.

Electron Microscopy

Thin-section studies of oocytes expressing Cx50. We focused on the organization of the plasma membrane and the neighboring protoplasmic region ("cortical" region). The plasma membrane of control oocytes contained numerous microvilli, folds, and invaginations that increased its surface area by approximately ninefold compared with a smooth spherical cell of similar diameter (Zampighi et al., 1995). The cytoplasm of the cortical region contained secretory granules closely associated with the plasma membrane (labeled "CG" in Fig. 4 A), small (~0.1 μm) and large (0.2–0.5 μm) diameter vesicles, mitochondria, and endoplasmic reticulum. Oocytes expressing high levels of Cx50, as assessed from the magnitude of I_{Cx50} and the density of the plasma membrane particles (see below), exhibited gap junctions that appeared as pentalamellar structures 16–18 nm in overall thickness (Figs. 4 B and 5 A). The gap junctions were either continuous ("reflective") or discontinuous ("annular") with the plasma membrane. Reflective gap junctions were formed by the association of the plasma membrane with a microvillus or a fold (Fig. 4 B), or in membrane invaginations (Fig. 5 A, closed arrow). Annular gap junctions appeared as vesicles in the cytoplasm and most likely originated from invaginations of the plasma membrane, which later pinched off into the cytoplasm (Fig. 4 B, △, and Fig. 5 A).

Freeze-fracture micrographs of the reflective and annular gap junctions revealed that the P face of the plasma membrane contained plaques of particles, and the complementary E (external) face contained the corresponding pits (Fig. 5 B). The plaques contained Cx50 hemichannels assembled into gap junctions. The height of the fracture step separating the junctional membranes (E-to-P transition, Fig. 5 B, open arrows) was 6–7 nm, and the extracellular space between the two membranes was 1–2 nm, which is consistent with that found in gap junctions. Annular gap junctions appeared as concave and convex surfaces with plaques of particles and complementary pits also separated by fracture steps of small height (Fig. 5 C).

Gap junctions were not observed in control oocytes (Fig. 4 A), in oocytes expressing low levels of Cx50 (<300 P face particles/μm^2), or in oocytes overexpressing other heterologous membrane proteins (in the absence of Cx50), such as the Na^+/glucose cotransporter (SGLT1), occludin, aquaporin-0, aquaporin-1, or *Shaker* K^+ channel. We have observed gap junction formation in oocytes expressing connexin46 (Zampighi, unpublished observations).

Freeze-fracture studies of oocytes expressing Cx50. In thin sections, oocytes expressing high levels of Cx50 were identified by the presence of gap junctions, which appeared 48–72 h after cRNA injection (Figs. 4 B and 5 A). In freeze fracture, expression of Cx50 was evident ~24 h after cRNA injection by the appearance of a distinct population of intramembrane particles in the

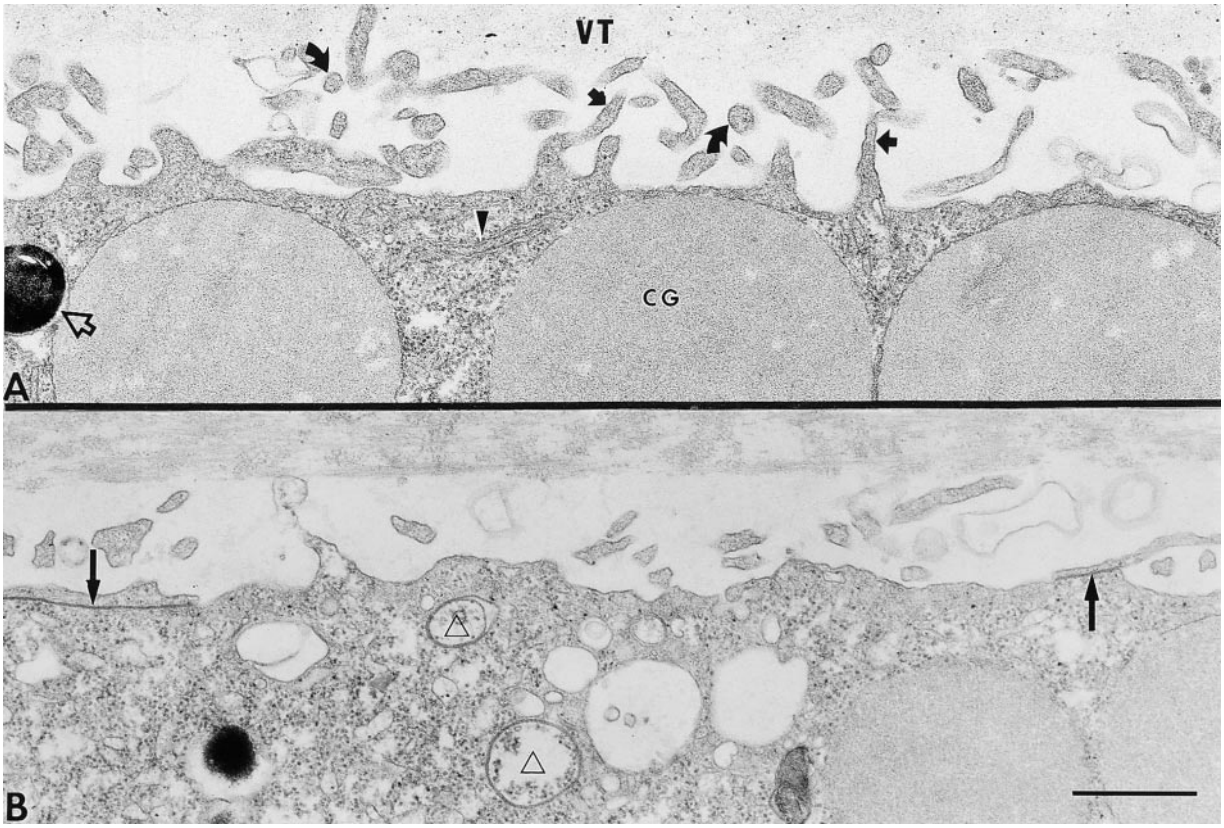

FIGURE 4. Thin section electron microscopy of cortical regions of a control oocyte and an oocyte expressing Cx50. (A) The vitelline membrane is represented by the gray region on top (VT). The plasma membrane contains folds and microvilli that are sectioned longitudinally (dark arrows) and transversely (curved arrows). The cytoplasm contains endoplasmic reticulum (arrowhead) and large cortical granules (CG). The open arrow points to a pigment granule present in the animal pole of *Xenopus laevis* oocytes. (B) Shown is the cortical region of an oocyte incubated for 3 d after Cx50 cRNA injection. Expression of Cx50 induced the formation gap junctions, which at this magnification appeared as dark lines (dark arrows and △). Gap junctions that were either continuous with the plasma membrane (reflective junctions; dark arrows) or were discontinuous with the plasma membrane (annular junctions) appeared as vesicles in the cytoplasm (△). Scale bar, 0.67 μm.

P face of the plasma membrane (Fig. 6). The newly inserted (Cx50) particles increased the density of particles in the P face, and the Cx50 particle density was correlated with the magnitude of I_{Cx50} (see Figs. 8 and 9).

To characterize the particles that appear after the expression of Cx50, we compared the size and shape of the P face particles in control oocytes and those expressing Cx50 using frequency histograms. In the P fracture face of control oocytes, ~93% of the endogenous proteins had a mean diameter of ~7.5 nm, and the rest had a mean diameter of ~11 nm (Eskandari et al., 1998). The density of the P face particle was 196 ± 9/μm² (mean ± SEM, n = 8). The complementary E face of the plasma membrane of control oocytes contained ~13-nm particles at a density approximately four times higher than the particle density in the P face (886 ± 36 particles/μm²). The density of the E face particles did not change after Cx50 expression.

The size (diameter) frequency histograms of the particles in oocytes expressing Cx50 exhibited a population of 9.0 ± 0.4 nm (mean ± SEM, n = 544) diameter particles (Fig. 7 A), in addition to the endogenous integral membrane proteins (hatched region in Fig. 7 A, and a smaller population at 11 nm). The newly inserted particles exhibited a symmetrical cross-sectional geometry that contrasted sharply with the size and shape of the endogenous particles (Fig. 6, A–G). When the density of the newly inserted particles reached 300–400/μm², they formed gap junction plaques (see below). Size frequency histograms also showed that the particle in the gap junction plaques exhibited the same size and shape as the newly inserted particle population (Fig. 7 B). Therefore, expression of Cx50 induced a population of intramembrane particles of distinct size and shape (hexamers), which assembled into plaques of complete channels (dodecamers) at a critical density.

We previously characterized the population of newly inserted P face particles induced by the expression of other heterologous membrane proteins, such as aquaporin-0, aquaporin-1, SGLT1, and opsin. Particle size

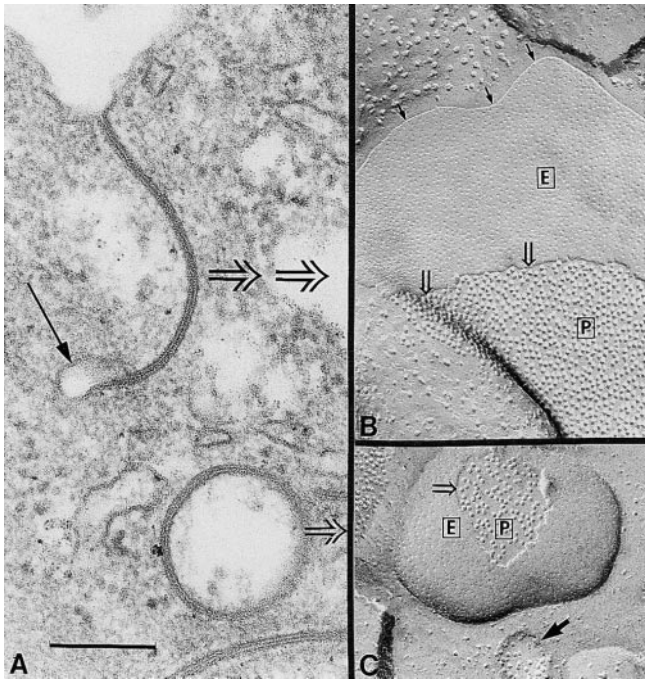

FIGURE 5. Thin section and freeze-fracture views of reflective and annular gap junctions formed in single oocytes expressing Cx50. (A) The reflective gap junction is formed in an invagination of the plasma membrane. This type of junction often terminates in a small clear vesicle (dark arrow). The annular gap junctions appear as vesicles formed by two closely apposed membranes enclosing a clear lumen. Chevron arrows point to the corresponding freeze-fracture views (in B and C) of the reflective and annular gap junctions. (B) In freeze fracture, the reflective gap junctions appear as plaques of particles (P) and complementary pits (E). The particles and pits forming the plaques are continuous with the fracture face of the nonjunctional plasma membrane, indicating that these arrays are part of the plasma membrane. The top shows a region containing the large (~13 nm diameter) endogenous particles characteristic of the E face of the plasma membrane of control oocytes. The furrow separating the junctional from the nonjunctional E faces (small dark arrows) is from an endogenous tight junction strand that is occasionally associated with the plasma membrane. Open arrows point to the step separating the E from the P face of the gap junctional plaque. The small height of the step (~6 nm) strongly indicates that the plaques of particles and pits represent gap junctions and not an arrangement of single hemichannels. (C) Shown are the fracture faces of an annular gap junction. The open arrow points to the fracture step separating the two faces. The dark arrow points to a small diameter vesicle containing hemichannels often found in the cytoplasm of oocytes expressing Cx50. Scale bar, 0.2 μm.

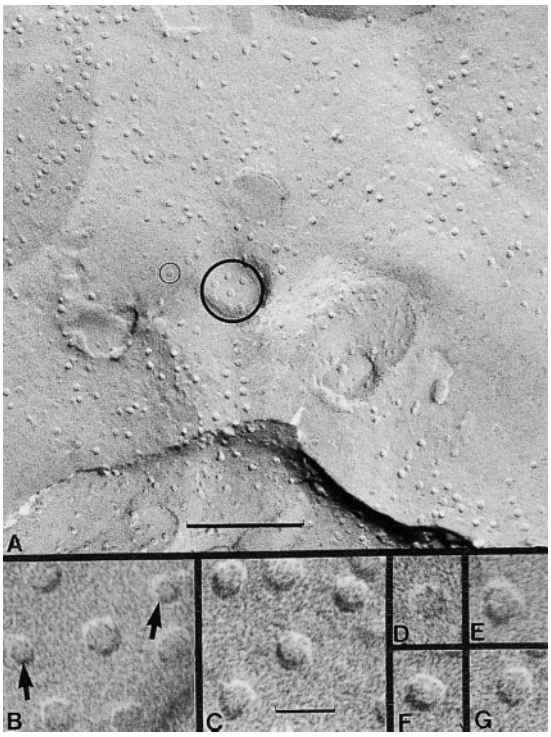

FIGURE 6. Comparison of the endogenous membrane proteins of the oocyte and the Cx50 hemichannels induced after cRNA injection. (A) A low magnification view of the plasma membrane of an oocyte expressing Cx50 is shown. This region of the plasma membrane was shadowed at a high angle to allow for the analysis of protein size and shape (see Fig. 7). The area enclosed by the large circle is shown in B and the particle in the small circle is shown in D. (B and C) Higher magnification views to show the difference between the smaller endogenous particles (arrows) and the larger Cx50 hemichannels. (D–G) Individual hemichannels were selected from the field in A and shown at high magnification to illustrate their rounded and polygonal overall shape. Scale bars: A, 0.16 μm; B–G, 16.6 nm.

analysis showed that each protein was represented by a particle with a distinct size and shape whose cross-sectional area predicts the number of alpha helices in the transmembrane domain (Eskandari et al., 1998). An analysis of the cross-sectional area of the particle induced after the expression of Cx50 predicted that each Cx50 particle could accommodate 24 ± 3 α helices (1.4 nm^2/helix; Eskandari et al., 1998). Therefore, based on the size and cross-sectional area of the particles, and their ability to form gap junctions, we conclude that Cx50 is inserted into the plasma membrane as hemichannels (hexamers).

The density of Cx50 hemichannels was correlated with I_{Cx50}. The density of Cx50 hemichannels in the P face (excluding those in gap junction plaques) was examined at various times after Cx50 cRNA injection (Fig. 8 and Table II). To relate the density measurements to functional ones, I_{Cx50} (at −50 mV and 10 μM $[Ca^{2+}]_o$) and C_m were also measured in the same oocytes (Table II).

Quantification of the P face particles in oocytes examined at different times after injection showed that the density of hemichannels was proportional to I_{Cx50} (Table II). At ~6 h after injection, the current was small (approximately −10 nA) and the density of particles did not increase significantly above that of endogenous particles measured in control oocytes (Fig. 8 B). At 24 h, the magnitude of I_{Cx50} increased to 415 nA and

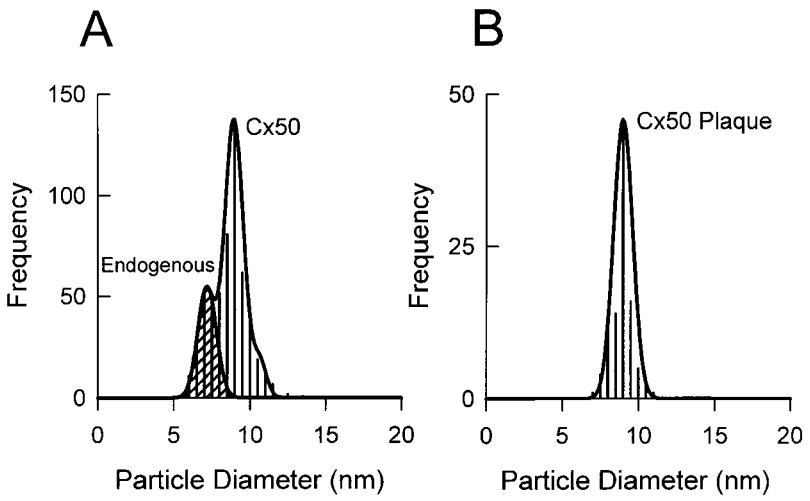

FIGURE 7. Size (diameter) frequency histograms of single intramembrane particles and those forming the gap junction plaques present in the P fracture face of oocytes expressing Cx50. (A) The histogram was constructed from 554 particle diameter measurements and included both the endogenous particles and the newly inserted hemichannels. The bin size was chosen to be 0.5 nm in size and the data in each bin are plotted at the center of the bin. The data were fitted with a multiple Gaussian function (smooth lines). The hatched region (particle size ~7 nm) and the larger particles (~11 nm) represent the endogenous oocyte P face particles (Eskandari et al., 1998). The prominent peak at 9.0 nm corresponds to Cx50 hemichannels. (B) A size frequency histogram constructed from 100 measurements of particles arranged in a gap junction plaque. The size of the particle is 9.0 nm, suggesting that this particle population is identical to the 9.0-nm particle identified in the analysis of single particles from nonplaque regions of the plasma membrane (A).

the hemichannel density to ~200/μm^2 above background (Fig. 8 C and Table II). At 48 h, I_{Cx50} and hemichannel density increased approximately twofold (Fig. 8 D and Table II). At this level of Cx50 expression, hemichannels assembled into gap junctions plaques of P face particles (Fig. 8, D and E, GJ). I_{Cx50} and the density of Cx50 hemichannels peaked at 72 h (Fig. 8 E and Table II); however, they decreased by ~25% with longer incubation times (Table II). The initial rate of Cx50 expression (Table III) indicates that hemichannels were inserted into the plasma membrane at a rate of 80,000 copies/s.

The area of the oocyte plasma membrane was estimated from whole-cell capacitance measurements (assuming 1 $\mu F/cm^2$; Table II), which together with I_{Cx50} (at −50 mV and 10 μM Ca^{2+}) obtained from the same oocyte, allowed for the calculation of the specific membrane conductance (in picosiemens per square micrometer). The specific membrane conductance plotted as a function of the Cx50 hemichannel density (per square micrometer) from the same oocytes, yielded a linear relationship, the slope (2.7×10^{-3} pS) of which corresponded to the product of the open probability (P_o) and the single channel conductance (γ) of the Cx50 hemichannel (Fig. 9).

Cx50 hemichannels assembled into gap junctions in single oocytes. Gap junction plaques were first observed 48 h after cRNA injection when Cx50 hemichannel density reached 300–400/μm^2 and, thereafter, occupied a fairly constant area of the plasma membrane (1.3–1.7%). At peak expression, the area covered by plaques contained $8.2–9.2 \times 10^9$ hemichannels; 35–40% of the total number of Cx50 hemichannels in the plasma membrane (~2.6×10^{10}; Table III).

Identification of intracellular vesicles containing Cx50 hemichannels. We took advantage of the distinct size and shape of the Cx50 hemichannel particles, as well as their ability to form gap junctions in single oocytes, to identify the vesicles involved in the insertion/retrieval pathway to and from the plasma membrane. Two types of vesicles within the cytoplasm contained hemichannels (Figs. 10–12). One was located close to the plasma membrane and to organelles such as the Golgi complex, the endoplasmic reticulum, and lysosomes (Figs. 10, A–D, and 12). These vesicles measured ~0.1 μm in diameter and contained slender projections, spaced ~20-nm apart, which protruded from the vesicle surface (Fig. 10 A, arrows). Some coated vesicles were

TABLE II

Electrophysiological and Morphological Data from Oocytes Expressing Connexin50

Oocyte*	Current	Conductance	Capacitance	Hemichannel density
	nA‡	*μS*§	*nF*	μm^{-2}‖
Control	5	0.2	363	0
6	−10	0.4	ND	BDL¶
24	−415	16.6	355	195 ± 13
48	−840	33.6	350	407 ± 36
72	−1160	46.4	313	537 ± 47
96	−865	34.6	261	442 ± 69

*The duration of incubation after cRNA injection is given in hours. ‡The whole-cell current was measured at −50 mV and 10 μM $[Ca^{2+}]_0$, and was corrected for the background oocyte current. §The whole-cell conductance was measured as a chord conductance at −50 mV. ‖The density of hemichannels (mean ± SEM) (excluding those in plaques) corresponds to the density of P face particles after correction for the density of the endogenous particles. ¶BDL, below detection level.

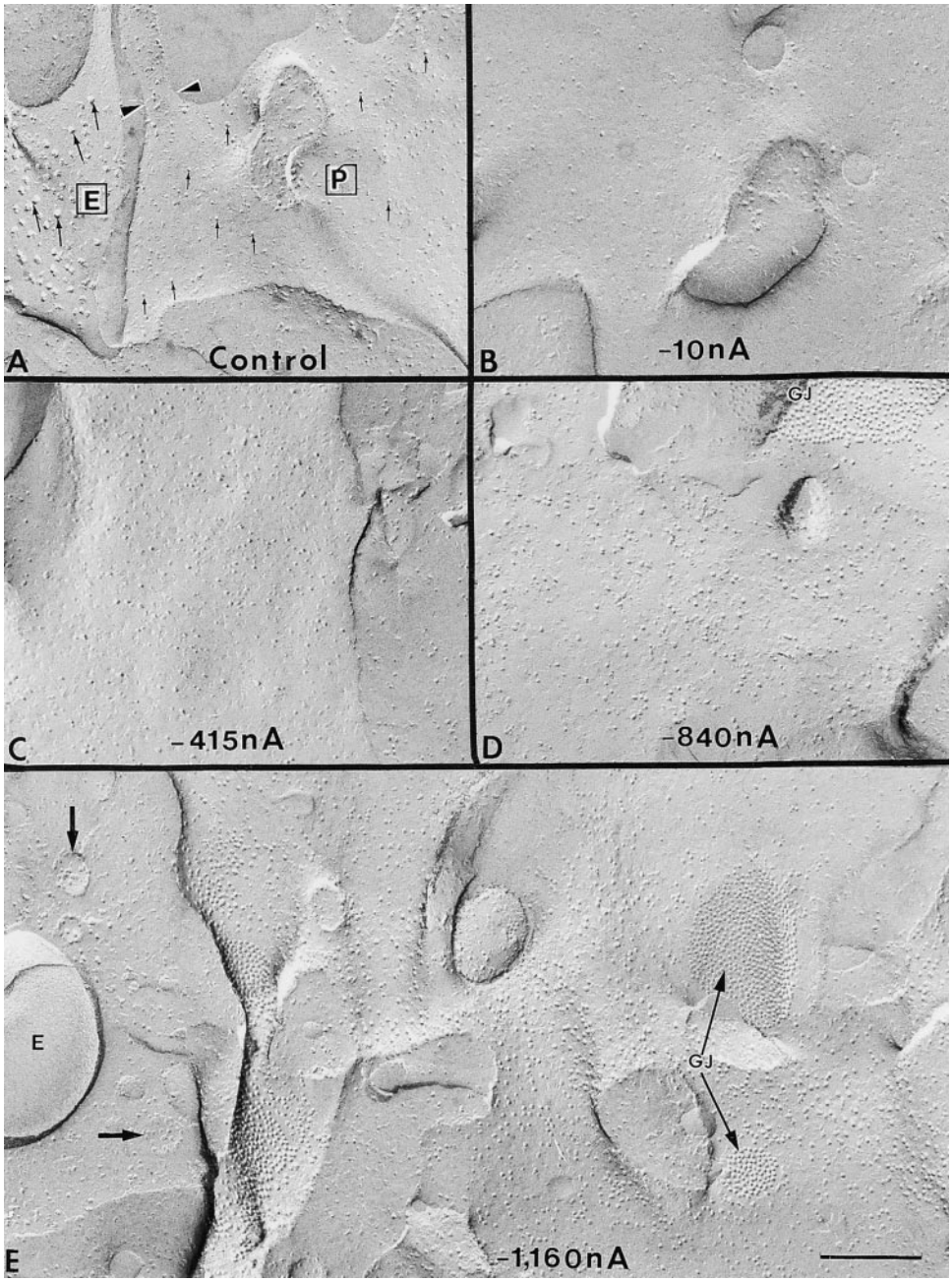

FIGURE 8. Comparison of the plasma membrane (P face) of a control oocyte with those of oocytes exhibiting different levels of Cx50 expression. (A) The P face (P) of control oocytes contains ~7-nm diameter particles (small arrows), and the E face (E) is characterized by the presence of 13-nm diameter particles (large arrows). The arrowheads point to the neck connecting a microvillus to the plasma membrane. (B–E) Both I_{Cx50} and the density of hemichannels were measured at various times after the injection of Cx50 cRNA; 6 h (B), 24 h (C), 48 h (D), and 72 h (E) (see also Table II). Expression of Cx50 increases the density of hemichannels only in the P face of the plasma membrane. The density of hemichannels is correlated with the magnitude of I_{Cx50}. The first indication of reflective gap junctions (GJ) was found 48 h after cRNA injection (D). Peak values for both I_{Cx50} and the particle density were seen at 72 h (E). In E, the upper left corner shows the convex surface (E) of an annular gap junction and the concave surface of the small vesicles (arrows) containing the characteristic Cx50 hemichannels. Scale bar, 0.2 μm.

fused with the plasma membrane through a narrow neck 25–30 nm in length and a diameter ranging from 20 to 40 nm (Fig. 10, B and C). In freeze fracture, these vesicles appeared as concave and convex surfaces and, depending on the expression level, contained 5–40 Cx50 hemichannels (Fig. 10, E–I). These vesicles also contained the 13-nm endogenous particles found on the E face.

The other type of vesicle with Cx50 hemichannels exhibited a larger diameter (0.2–0.5 μm) and an irregular shape (Figs. 11 and 12). Markers of the extracellular space, such as peroxidase, showed electron-dense reaction products in the lumen of these vesicles (Fig. 13). Therefore, the larger vesicles were either connected to the extracellular space or originated from invaginations of the plasma membrane that ultimately pinched off into the cytoplasm (Fig. 11 A).

In freeze fracture, the large vesicles were characterized by the presence of Cx50 hemichannels; i.e., 9-nm particles in the P face and the complementary pits in the E face (Fig. 12). Some large vesicles contained hemichannels at a density similar to that in the gap junction plaques described in the plasma membrane (Figs. 11 C and 12, A and B), and most likely correspond to the annular gap junction seen in thin sections (Figs. 4 B and 5 A). Other large vesicles contained

table iii

Quantification of Connexin50 Hemichannels in the Plasma Membrane

Oocyte*	Total area of the plasma membrane	Percent area covered by plaques§	Number of hemichannels (single)‖	Number of hemichannels (in plaques)¶	Total number of hemichannels**
	μm^2‡				
24	3.5×10^7	0	0.7×10^{10}	0	0.7×10^{10}
48	3.5×10^7	1.3	1.4×10^{10}	8.4×10^9	2.3×10^{10}
72	3.1×10^7	1.6	1.7×10^{10}	9.2×10^9	2.6×10^{10}
96	2.6×10^7	1.7	1.2×10^{10}	8.2×10^9	2.0×10^{10}

*The duration of incubation after cRNA injection is given in hours. ‡The area of the plasma membrane was estimated from the oocyte capacitance (using 1 $\mu F/cm^2$) (Table II). §The percentage area covered by gap junction plaques was estimated from the fraction of the area occupied by plaques in 100 μm^2 of P face of the plasma membrane (see MATERIALS and METHODS). ‖The number of single hemichannels was the product of the mean density of Cx50 P face particles times the total area of the plasma membrane. ¶The number of cell-to-cell channels in the reflective gap junctions was the product of the total area of the plasma membrane, the fractional area covered by plaques, the mean density of hemichannels in plaques, and two (see MATERIALS and METHODS). **The total number of hemichannels was the sum of the single particles plus the particles in gap junction plaques.

hemichannels at lower densities or in small clusters located in highly curved regions of the vesicle (Fig. 12, A, C, and D). These large vesicles may correspond to early endosomes or the trans-Golgi network.

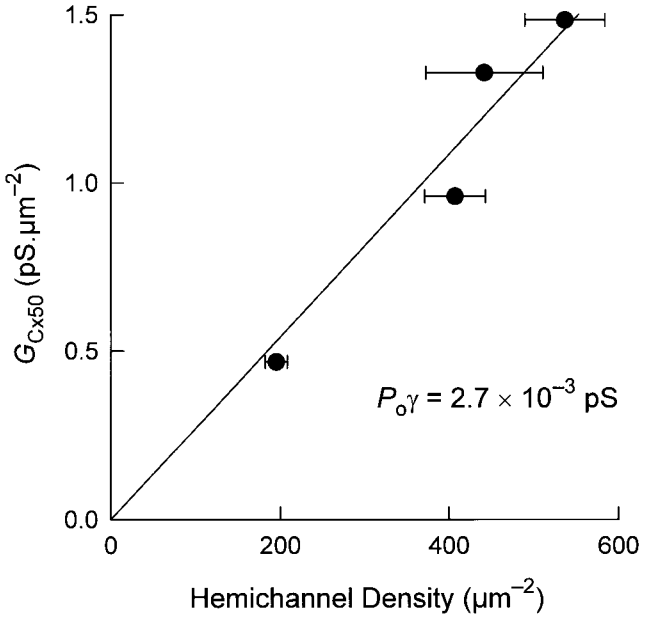

FIGURE 9. Estimation of the unitary properties of Cx50 hemichannels. Hemichannel density (per square micrometer) was determined in oocytes expressing different levels of Cx50, and the density due to the endogenous proteins was subtracted. The density of the particles reported here does not include those in the plaque regions, as these do not contribute to I_{Cx50}. The membrane conductance due to Cx50 was determined at −50 mV and 10 µM $[Ca^{2+}]_o$ as a chord conductance according to $G_{Cx50} = I_{Cx50}/(V - V_{rev})$. Background conductance was subtracted in the presence of 5 mM $[Ca^{2+}]_o$. Membrane capacitance was used to determine membrane surface area using 1 $\mu F/cm^2$, which allows the calculation of the specific membrane conductance (picosiemens per square micrometer). Each data point represents the membrane conductance and hemichannel density in the same oocyte. The straight line is linear regression through the data, and the slope corresponds to a Cx50 open probability multiplied by the single channel conductance ($P_o\gamma$).

The E fracture face of the vesicles provided another important clue regarding their origin. These faces contained the complementary pits of the Cx50 hemichannels at a density similar to plaques (Fig. 12 E), or arranged in small clusters (Fig. 12 E, □). In addition to the hemichannels, the E face of the large vesicles also contained large 13-nm-diameter particles (Fig. 12 E, arrows). These E face particles correspond to a population of endogenous proteins in the plasma membrane of control oocytes (Zampighi et al., 1995). Therefore, the vesicles identified in this study contained Cx50 hemichannels intermingled with endogenous proteins of the oocyte plasma membrane, suggesting that trafficking of endogenous and heterologous proteins uses a common pathway.

discussion

Injection of Cx50 cRNA into oocytes leads to the appearance of a new population of particles (Cx50 hemichannels) in the plasma membrane, whose density is directly correlated with a whole-cell Ca^{2+}-sensitive current (I_{Cx50}). Several observations suggest that the newly inserted particles represent Cx50 hemichannels, and that I_{Cx50} is in fact mediated by Cx50 hemichannels. First, the newly inserted particles exhibited a circular geometry with a diameter of 6.5 ± 0.5 nm (after correcting for the thickness of the platinum-carbon film; 2.4 nm) (Eskandari et al., 1998). The cross-sectional area, 34 ± 4 nm^2 (πr^2), can accommodate 24 ± 3 α helices (Eskandari et al., 1998). Both the particle diameter and the cross-sectional area observed here are consistent with the reported values from two-dimensional crystals of gap junction membrane channels (Unger et al., 1997), and ordered arrays of hemichannels (Perkins et al., 1997). The size and shape of the Cx50 particle suggest a hexameric hemichannel composed of four α helices per subunit.

Second, at a density of 300–400/μm^2, Cx50 particles formed reflective gap junctions in the plasma mem-

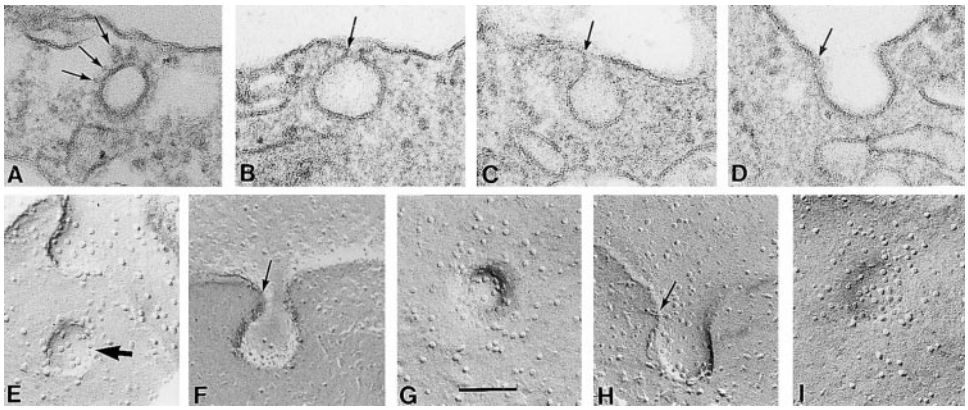

FIGURE 10. Thin section and freeze-fracture electron microscopy of small vesicles containing Cx50 hemichannels. (A) A small vesicle (~90 nm in diameter) is shown in the cytoplasm just underneath the plasma membrane. The vesicle is composed of a lipid bilayer from which slender projections (~15 nm in length) extend into the cytoplasm (small arrows). Similar vesicles were also present in control oocytes but lacked hemichannels. B–D show various stages of the fusion of the small vesicles with the cytoplasm. The vesicles were connected to the plasma membrane through stalks 22–30 nm in length and of variable diameter (B and C, arrows). (D) After fusion, the vesicle remained as a depression in the plasma membrane. (E–I) In freeze fracture, the vesicles contained the characteristic hemichannels (concave face). The vesicles were present in the cytoplasm (E, dark arrow) and fused with the plasma membrane through a stalk 20–25 nm in length (F and H, arrows). Views from the plane of the plasma membrane (G and I) show the complex formed by the fused vesicle (containing the Cx50 hemichannels) and the plasma membrane. Scale bar, 0.1 μm.

brane of single oocytes. This property has not been observed for endogenous proteins in control oocytes, or in oocytes expressing a wide variety of other heterologous membrane proteins.

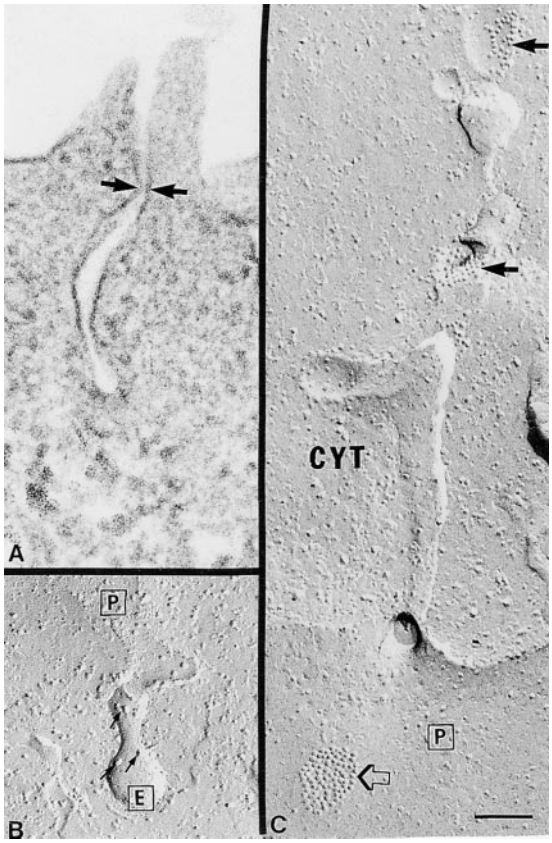

FIGURE 11. Thin section and freeze-fracture electron microscopy of invaginations of the plasma membrane containing Cx50 hemichannels. (A) Thin section of an infolding (~0.3 μm in length) of the plasma membrane that ended in a small rounded vesicle. Regions of close membrane apposition often occurred near the plasma membrane (arrows). Similar structures were also observed in control oocytes. (B) Freeze-fracture view of an invagination of the plasma membrane that also ended in a round vesicle of ~100 nm in diameter. The convex E face (E) of the vesicle exhibited pits complementary to the Cx50 hemichannels, and also contained the endogenous 13-nm diameter particles (small dark arrows). (C) Freeze-fracture view of a long tubular invagination continuous with the plasma membrane. The plasma membrane P face (P) contained single as well as plaques of Cx50 hemichannels (open arrow). Similarly, the invagination contained both single hemichannels and hemichannels in plaques (dark arrows). CYT, cytoplasm. Scale bar, 0.1 μm.

Third, oocytes expressing Cx50 demonstrated a current (I_{Cx50}) that was activated at low $[Ca^{2+}]_o$. The properties of I_{Cx50} suggest that it is mediated by a nonselective cation channel. I_{Cx50} could be blocked by octanol or intracellular acidification, other characteristics of gap-junction channels and hemichannels (e.g., Li et al., 1996; Steiner and Ebihara, 1996; Trexler et al., 1998; Wang and Peracchia, 1998).

Finally, at low $[Ca^{2+}]_o$ and large voltage steps, there was a time-dependent inactivation of Cx50 macroscopic currents, such that the steady state I–V relationship displayed regions of negative slope. Similar voltage-dependent characteristics have been observed for other connexin hemichannels (DeVries and Schwartz, 1992; Ebihara and Steiner, 1993; Ebihara et al., 1999).

Altogether, the functional, pharmacological, and morphological characteristics observed in Cx50-expressing oocytes point to the expression of connexin hemichannels.

Estimation of Cx50 Unitary Properties

A unique aspect of this study was that the total number of hemichannels inserted into the plasma membrane was estimated in the same oocytes in which I_{Cx50} was measured. This allowed us to estimate the unitary properties of Cx50 hemichannels.

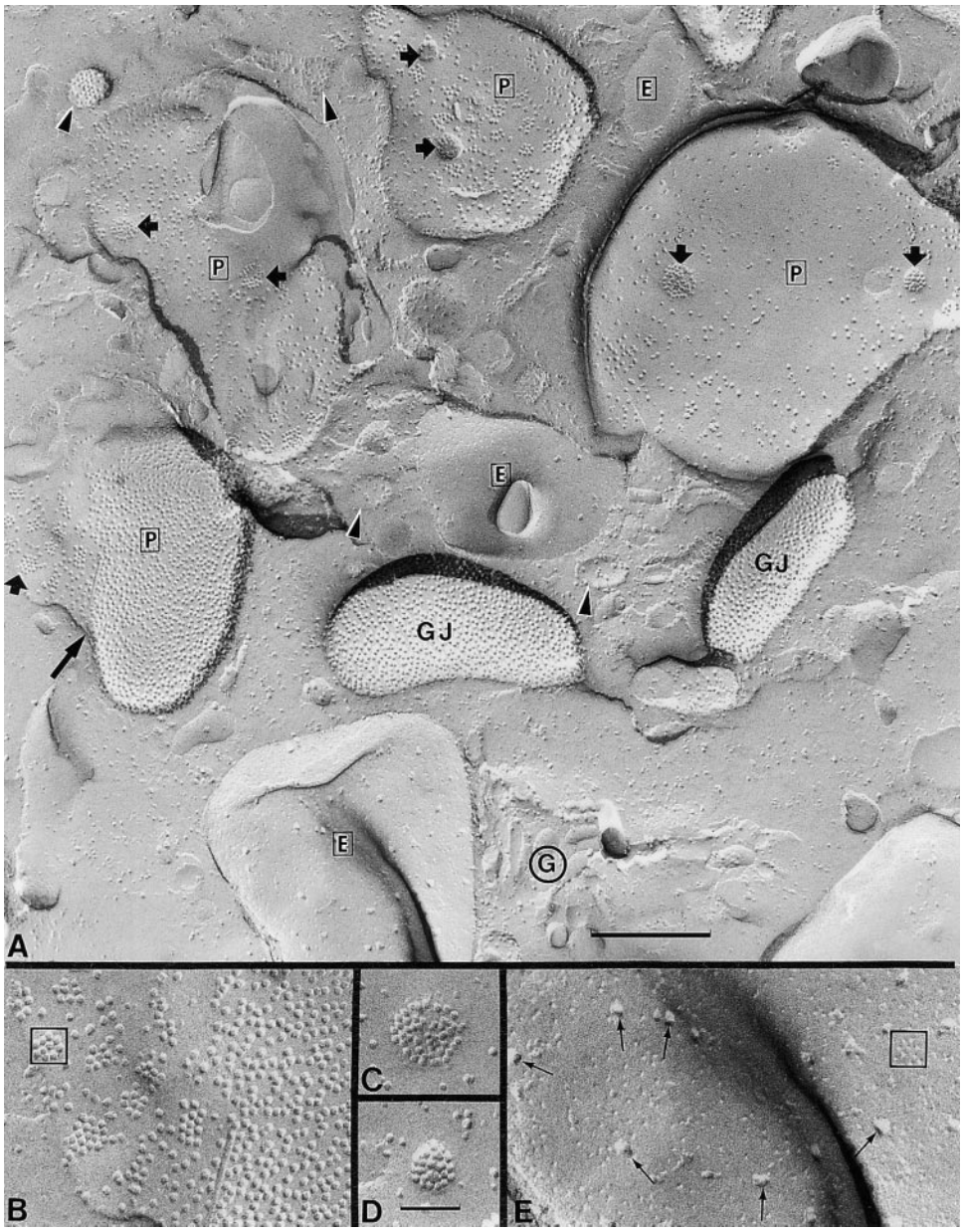

FIGURE 12. Freeze-fracture electron microscopy of vesicles containing hemichannels located deep in the cytoplasm of an oocyte expressing Cx50. (A) Several large vesicles are shown with the characteristic hemichannels in the P face (P and GJ), and the complementary pits in the E face (E). Some vesicles contain hemichannels at high or low densities and often both types of arrangements are observed in the same vesicle. Vesicles with a high density of particles formed plaques similar to those formed by reflective gap junctions in the plasma membrane (GJ). Vesicles containing low densities of hemichannels exhibited small round plaques (dark arrows), which were often located in a highly curved region of the membrane. The E faces (E) contained the endogenous 13-nm diameter particles intermingled with the complementary pits of hemichannels. G refers to the Golgi stacks. (B) A higher magnification view of a vesicle exhibiting single hemichannels, and hemichannels arranged in rosettes (□) and plaques. C and D show higher magnification views of the small plaques seen in large vesicles with a lower density of Cx50 hemichannels. (E) A higher magnification view of the E face of the vesicle at the bottom of A. The small arrows point to the 13-nm diameter endogenous E face particles and □ encloses a rosette of pits complementary to the small plaques of hemichannels seen in vesicles with a lower density of hemichannels (as in C and D). Scale bars: A, 0.26 μm; B–E, 66 nm.

The increase in membrane conductance due to expression of Cx50 hemichannels (G_{Cx50}) is proportional to the number of hemichannels (n), the single hemichannel conductance (γ), and the channel open probability (P_o) ($G_{Cx50} = P_o\,\gamma\,n$). Combined freeze-fracture electron microscopy and electrophysiological measurements were used to determine the total number of hemichannels (n) and the membrane conductance (G_{Cx50}) in the same oocytes. At −50 mV and 10 μM $[Ca^{2+}]_o$, $P_o\,\gamma$ for Cx50 hemichannels was -2.7×10^{-3} pS (Fig. 9). Using 30 pS for Cx50 single channel conductance (obtained under physiological extracellular and intracellular Na^+ and K^+ concentrations and symmetrical 100 nm $[Ca^{2+}]$; Eskandari, S., and D.D.F. Loo, manuscript in preparation), we estimate that at 10 μM $[Ca^{2+}]_o$, Cx50 P_o is -9×10^{-5}; i.e., only ~1 in 10,000 hemichannels is open at any given time. In light of the observed Ca^{2+} sensitivity of G_{Cx50}, we predict that Cx50 hemichannels would rarely open at physiological $[Ca^{2+}]_o$ (1–2 mM). These data suggest that the whole-cell conductance induced at peak expression by lowering $[Ca^{2+}]_o$ to 10 μM (46 μS; Table II) results from the opening of $\sim 1.5 \times 10^6$ hemichannels (γ = 30 pS), representing ~0.009% of the total number of single hemichannels in the plasma membrane (1.7×10^{10}; Table III). This suggests that, in the oocyte, there is one conducting hemichannel every ~20 μm² of the plasma membrane. At a more physiological $[Ca^{2+}]_o$ (1–2 mM),

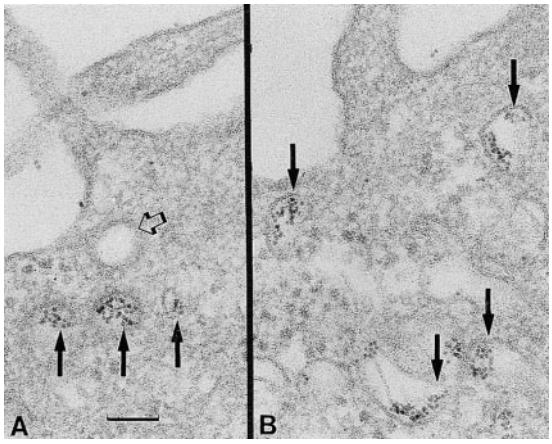

FIGURE 13. Thin sections of the cortical regions of oocytes incubated in the presence of the enzyme peroxidase. (A) The peroxidase enzymatic products are shown in the lumen (dark arrows) of three vesicles. The open arrow points to a smaller coated vesicle without the marker. B shows several irregularly shaped vesicles (arrows) containing peroxidase reaction products in their lumens. The intraluminal localization of the extracellular marker suggests that these vesicles are derived from the plasma membrane of the oocyte by endocytosis. Scale bar, 0.1 μm.

G_{Cx50} decreases by ≥20-fold, which would correspond to one open hemichannel for every ~400 μm^2 of the plasma membrane. If these findings in oocytes are extrapolated to a smaller cell, such as a liver hepatocyte, and a density of 500 hemichannels/μm^2 is assumed, we estimate that there would be two conducting hemichannels per cell. Therefore, our data suggest that at physiological $[Ca^{2+}]_o$, Cx50 hemichannels play a small role in single cell permeability and homeostasis, and the potential physiological significance of this hemichannel would be confined to large cells possessing a high density of hemichannels, conditions which favor channel opening (e.g., low $[Ca^{2+}]_o$), or pathophysiological states that may result in apoptosis.

Trafficking of Cx50

After Cx50 cRNA injection, the total number of hemichannels in the plasma membrane reached a steady state ($2.3–2.6 \times 10^{10}$) at 72 h (Table II), which correlated with the electrophysiological assay of hemichannel function (Figs. 3 and 8). Based on the number of hemichannels in the oocyte plasma membrane 24 h after cRNA injection (Table II), the initial insertion rate of Cx50 into the plasma membrane was ~80,000 hemichannels/s. The observation that Cx50 hemichannels were colocalized in the same vesicles with endogenous proteins of the oocyte suggests that Cx50 overexpression does not alter the oocyte's constitutive translation and trafficking machinery.

Assuming that insertion is via fusion of the small coated vesicles (0.1 μm diameter) with the plasma membrane, and that each vesicle contains 5–40 Cx50 hemichannels, we predict that Cx50 over-expression should increase the plasma membrane by 63–503 $\mu m^2/s$ ($5.4–43.4 \times 10^6$ μm^2 in 24 h). In spite of such a sizable rate of insertion, there was no increase in the area of the plasma membrane (Fig. 3; Table III). Thus, exocytosis was balanced by endocytosis. It is interesting to note that at peak Cx50 expression, these rates of exocytosis and endocytosis would lead to the replacement of the entire plasma membrane of the oocyte in ~24 h!

In contrast, expression of other heterologous membrane proteins such as SGLT1 (Zampighi et al., 1995; Hirsch et al., 1996) and aquaporin-0 (Chandy et al., 1997) increased the area of the plasma membrane of oocytes up to fourfold. In the case of SGLT1, the increase in the plasma membrane area occurs concurrently with an increase in the number of transporters in the plasma membrane, and the rate of SGLT1 insertion is comparable to that observed here (Hirsch et al., 1996; Wright et al., 1997). Therefore, it appears that the delivery of some endogenous membrane proteins, as well as heterologous proteins such as SGLT1 and Cx50, to the plasma membrane involves the same mechanism. The difference in the trafficking of the heterologous membrane proteins appears to involve the retrieval mechanism. In the case of Cx50, endocytosis of large Cx50-containing vesicles balances the rate of small vesicle insertion. In oocytes expressing SGLT1, however, this pathway does not balance the rate of vesicle exocytosis, resulting in a continuous increase in the area of the plasma membrane.

Cx50 was inserted into the plasma membrane as functional hemichannels. No gap junctions were observed until the density of hemichannels in the plasma membrane reached a threshold of 300–400/μm^2. Therefore, the plaques of channels were assembled from the recruitment of the Cx50 hemichannels in the plasma membrane. Once maximal expression levels were reached, the fraction of hemichannels in nonjunctional and junctional membrane regions remained relatively constant (Table III), indicating that there was a steady state between the insertion of hemichannels into the plasma membrane and their entry into junctional plaques. Retrieval occurred through endocytosis of both hemichannels and complete channels assembled in junctional plaques (see below). Assuming a steady state at maximal expression levels (72 h), we estimate that the half-life of a single hemichannel (junctional and nonjunctional combined) in the plasma membrane was ~3.7 d. This is longer than the metabolic half-life estimated for other connexins in other expression systems (<5 h; e.g., Fallon and Goodenough, 1981; Beardslee et al., 1998).

We identified Cx50 hemichannels in small (~100 nm) and large (0.2–0.5 μm) diameter vesicles. We in-

terpret these vesicles as components of the trafficking machinery involved in Cx50 insertion into and retrieval from the plasma membrane. Three observations suggested that the larger vesicle originates from plasma membrane invaginations and is a component of the retrieval pathway. First, when the hemichannel density reached 300–400 μm^2 in the plasma membrane, the invaginations assembled gap junctions that pinched off and appeared as annular gap junctions in the cytoplasm (Figs. 4 B, 5 A, and 11 A; Larsen et al., 1979). Second, the extracellular marker, peroxidase, labeled the lumen of the large, but not the small, vesicles. Third, these larger vesicles contained hemichannels intermingled with an endogenous plasma membrane protein of the oocyte (i.e., the 13-nm particle in the E face). Altogether, these results suggest that Cx50 hemichannel retrieval shares a pathway with endogenous proteins of the plasma membrane of the oocyte. In this scheme, the large vesicles represent early endosomes formed by endocytosis of large invaginations of the plasma membrane.

The origin and fate of the smaller coated vesicles containing the hemichannels were difficult to determine. One possibility is that they insert the hemichannels into the plasma membrane, as their lumen was not observed to be labeled with peroxidase. This interpretation is likely because these vesicles were observed to be associated with Golgi-resembling flattened membrane sacs. An alternative possibility is that the coated vesicle is involved in the endocytosis of hemichannels only (not gap junctions) from the plasma membrane, and subsequently delivers them to an early endosomal compartment. While additional information will be required to distinguish between the two hypotheses, our

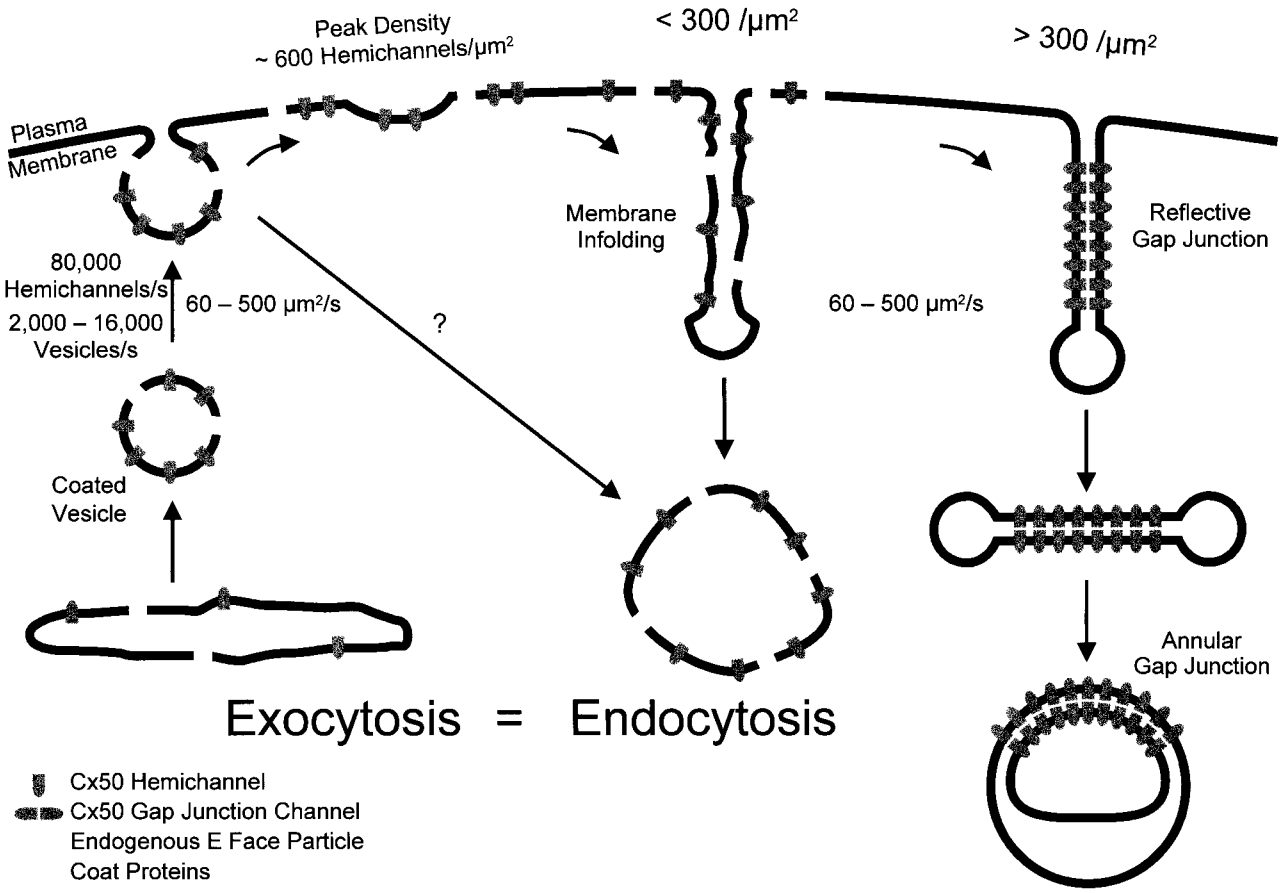

FIGURE 14. A model proposing that the trafficking of Cx50 hemichannels to and from the plasma membrane of oocytes occurs along the constitutive (default) pathway. We propose that Cx50 is inserted into the plasma membrane as a hemichannel (connexin hexamer). Insertion into the plasma membrane occurs at an initial rate of 80,000 hemichannels/s. Hemichannel insertion is via exocytosis of small coated vesicles at a rate of 2,000–16,000 vesicles/s, corresponding to the addition of 63–503 μm^2/s of membrane to the plasma membrane. Retrieval occurs through the formation of membrane invaginations that eventually pinch off and form large vesicles in the cytoplasm. At a hemichannel density $<300/\mu m^2$, the Cx50 hemichannels are retrieved, intermingled with some endogenous plasma membrane proteins, in the same large vesicles. At a density >300 hemichannels/μm^2, the large vesicles form reflective gap junctions that pinch off and appear as annular gap junctions in the cytoplasm. The principal characteristic of this pathway is that the area of the plasma membrane does not change during hemichannel insertion, indicating that plasma membrane endocytosis balances the rate of vesicle insertion.

identification of vesicles containing hemichannels represents a necessary first step for a more accurate description of the trafficking of heterologous proteins to and from the plasma membrane of oocytes.

In summary, our results led to the hypothesis that Cx50 hemichannel insertion into the plasma membrane was via exocytosis of small coated vesicles (Fig. 14). This pathway was shared by both endogenous and Cx50 proteins. This process steadily increased the density of Cx50 hemichannels in the plasma membrane until a steady state level was reached at 72 h. Retrieval of Cx50 hemichannels from the plasma membrane occurred via endocytosis of large vesicles. At low density ($<300/\mu m^2$), retrieval of hemichannels started in invaginations of the plasma membrane that pinched off and formed large cytoplasmic vesicles. This pathway was also shared by both endogenous and Cx50 proteins. At higher densities ($>300/\mu m^2$), the large invaginations formed reflective gap junctions that pinched off and appeared as annular gap junctions in the cytoplasm. The principal characteristic was that, despite the ongoing insertion and retrieval processes, the area of the plasma membrane remained constant.

We thank Dr. D.L. Paul (Harvard Medical School, Cambridge, MA) for kindly providing the plasmid containing the Cx50 cDNA. The assistance of Nancy Olea, Manuela Contreras, and Daisy Leung is greatly appreciated.

This work was supported by grants EY-04410, DK-41301, NS-25554, and DK-19567 from the National Institutes of Health.

Original version received 14 December 1998 and accepted version received 22 February 1999.

references

Beardslee, M.A., J.G. Laing, E.C. Beyer, and J.E. Saffitz. 1998. Rapid turnover of connexin43 in the adult rat heart. *Circ. Res.* 83:629–635.

Chandy, G., G.A. Zampighi, M. Kreman, and J.E. Hall. 1997. Comparison of the water transporting properties of MIP and AQP1. *J. Membr. Biol.* 159:29–39.

Dahl, G., T. Miller, D. Paul, R. Voellmy, and R. Werner. 1987. Expression of functional cell–cell channels from cloned rat liver gap junction complementary DNA. *Science.* 236:1290–1293.

DeVries, S.H., and E.A. Schwartz. 1992. Hemi-gap-junction channels in solitary horizontal cells of the catfish retina. *J. Physiol. (Camb.).* 445:201–230.

Ebihara, L. 1996. *Xenopus* connexin38 forms hemi-gap-junctional channels in the nonjunctional plasma membrane of *Xenopus* oocytes. *Biophys. J.* 71:742–748.

Ebihara, L., V.M. Berthoud, and E.C. Beyer. 1995. Distinct behavior of connexin56 and connexin46 gap junctional channels can be predicted from the behavior of their hemi-gap-junctional channels. *Biophys. J.* 68:1796–1803.

Ebihara, L., and E. Steiner. 1993. Properties of a nonjunctional current expressed from a rat connexin46 cDNA in *Xenopus* oocytes. *J. Gen. Physiol.* 102:59–74.

Ebihara, L., X. Xu, C. Oberti, E.C. Beyer, and V.M. Berthoud. 1999. Co-expression of lens fiber connexins modifies hemi-gap-junctional channel behavior. *Biophys. J.* 76:198–206.

Eskandari, S., E.M. Wright, M. Kreman, D.M. Starace, and G.A. Zampighi. 1998. Structural analysis of cloned plasma membrane proteins by freeze-fracture electron microscopy. *Proc. Natl. Acad. Sci. USA.* 95:11235–11240.

Fallon, R.F., and D.A. Goodenough. 1981. Five-hour half-life of mouse liver gap-junction protein. *J. Cell Biol.* 90:521–526.

Findlay, I., M.J. Dunne, and O.H. Petersen. 1985. High-conductance K^+ channel in pancreatic islet cells can be activated and inactivated by internal calcium. *J. Membr. Biol.* 83:169–175.

Gupta, V.K., V.M. Berthoud, N. Atal, J.A. Jarillo, L.C. Barrio, and E.C. Beyer. 1994. Bovine connexin44, a lens gap junction protein: molecular cloning, immunologic characterization, and functional expression. *Invest. Ophthalmol. Vis. Sci.* 35:3747–3758.

Hirsch, J.R., D.D.F. Loo, and E.M. Wright. 1996. Regulation of the Na^+/glucose cotransporter expression by protein kinases in *Xenopus laevis* oocytes. *J. Biol. Chem.* 271:14740–14746.

Johnston, M.F., S.A. Simon, and F. Ramón. 1980. Interaction of anaesthetics with electrical synapses. *Nature.* 286:498–500.

Larsen, W.J., H.-N. Tung, S.A. Murray, and C.A. Swenson. 1979. Evidence for the participation of actin microfilaments and bristle coats in the internalization of gap junction membrane. *J. Cell Biol.* 83:576–587.

Li, H., T.-F. Liu, A. Lazrak, C. Peracchia, G.S. Goldberg, P.D. Lampe, and R.G. Johnson. 1996. Properties and regulation of gap junctional hemichannels in the plasma membranes of cultured cells. *J. Cell Biol.* 134:1019–1030.

Loo, D.D.F., A. Hazama, S. Supplisson, E. Turk, and E.M. Wright. 1993. Relaxation kinetics of the Na^+/glucose cotransporter. *Proc. Natl. Acad. Sci. USA.* 90:5767–5771.

Parent, L., S. Supplisson, D.D.F. Loo, and E.M. Wright. 1992. Electrogenic properties of the cloned Na^+/glucose cotransporter. I. Voltage-clamp studies. *J. Membr. Biol.* 125:49–62.

Paul, D.L., L. Ebihara, L.J. Takemoto, K.I. Swenson, and D.A. Goodenough. 1991. Connexin46, a novel lens gap junction protein, induces voltage-gated currents in nonjunctional plasma membrane of *Xenopus* oocytes. *J. Cell Biol.* 115:1077–1089.

Perkins, G., D. Goodenough, and G. Sosinsky. 1997. Three-dimensional structure of the gap junction connexon. *Biophys. J.* 72: 533–544.

Reifarth, F.W., S. Amasheh, W. Clauss, and W.-M. Weber. 1997. The Ca^{2+}-inactivated Cl^- channel at work: selectivity, blocker kinetics and transport visualization. *J. Membr. Biol.* 155:95–104.

Spray, D.C., and J.M. Burt. 1990. Structure–activity relations of the cardiac gap junction channel. *Am. J. Physiol.* 258:C195–C205.

Steiner, E., and L. Ebihara. 1996. Functional characterization of canine connexin45. *J. Membr. Biol.* 150:153–161.

Trexler, E.B., M.V.L. Bennett, T.A. Bargiello, and V.K. Verselis. 1996. Voltage gating and permeation in a gap junction hemichannel. *Proc. Natl. Acad. Sci. USA.* 93:5836–5841.

Trexler, E.B., M.V.L. Bennett, T.A. Bargiello, and V. Verselis. 1998. Studies of gating in Cx46 hemichannels. *In* Gap Junctions. R. Werner, editor. IOS Press, Amsterdam, Netherlands. 55–59.

Unger, V.M., N.M. Kumar, N.B. Gilula, and M. Yeager. 1997. Projection structure of a gap junction membrane channel at 7 Å resolution. *Nat. Struct. Biol.* 4:39–43.

Wang, X.G., and C. Peracchia. 1998. Chemical gating of heteromeric and heterotypic gap junction channels. *J. Membr. Biol.* 162: 169–176.

Weber, W.-M., K.M. Liebold, F.W. Reifarth, and W. Clauss. 1995. The Ca^{2+}-induced leak current in *Xenopus* oocytes is indeed mediated through a Cl^- channel. *J. Membr. Biol.* 148:263–275.

Werner, R., T. Miller, R. Azarnia, and G. Dahl. 1985. Translation and functional expression of cell–cell channel mRNA in *Xenopus* oocytes. *J. Membr. Biol.* 87:253–268.

White, T.W., R. Bruzzone, D.A. Goodenough, and D.L. Paul. 1992. Mouse Cx50, a functional member of the connexin family of gap junction proteins, is the lens fiber protein MP70. *Mol. Biol. Cell.* 3:711–720.

Wright, E.M., J.R. Hirsch, D.D.F. Loo, and G.A. Zampighi. 1997. Regulation of Na^+/glucose cotransporters. *J. Exp. Biol.* 200:287–293.

Zampighi, G., M. Kreman, F. Ramón, A.L. Moreno, and S.A. Simon. 1988. Structural characteristics of gap junctions. I. Channel number in coupled and uncoupled conditions. *J. Cell Biol.* 106:1667–1678.

Zampighi, G.A., M. Kreman, K.J. Boorer, D.D.F. Loo, F. Bezanilla, G. Chandy, J.E. Hall, and E.M. Wright. 1995. A method for determining the unitary functional capacity of cloned channels and transporters expressed in *Xenopus laevis* oocytes. *J. Membr. Biol.* 148:65–78.

Zhang, Y., D.W. McBride, Jr., and O.P. Hamill. 1998. The ion selectivity of a membrane conductance inactivated by extracellular calcium in *Xenopus* oocytes. *J. Physiol. (Camb.).* 508:763–776.